

Dipolar models of ferromagnet particles interaction in magnetorheological composites

A. M. BILLER^a, O. V. STOLBOV^{a,b}, YU. L. RAIKHER^{a,b}

^a*Institute of Continuous Media Mechanics, Russian Academy of Sciences, Ural Branch, Perm, 614013, Russia*

^b*Perm National Research Polytechnic University, Perm, 614990, Russia*

Magnetorheological (MR) suspensions and polymers are filled with microparticles of magnetically soft (magnetizable) ferromagnet or ferrite. A single filler particle under an applied field magnetizes virtually uniformly being a member of an assembly, as in a MR system, the particle, along with the external field, experiences the action of the fields induced by its neighbors. In result, the particle magnetization becomes non-uniform, and this fact strongly affects the attraction/repulsion interparticle forces. Because of that, all the dipole models, where the particles of finite size are replaced by point magnetic moments, are by definition approximate. However, they are widely in use due to their simplicity. In the present paper, in the framework of a two-particle problem we estimate the limits of applicability of the known dipole approximations of interparticle interaction and propose a new one, termed *the nonlinear interacting dipole* model. The advantage of the latter is that it accounts for the restrictions imposed on interparticle forces by the magnetic saturation of filler particles (e.g. iron) in real MR composites.

(Received May 7, 2015; accepted June 25, 2015)

Keywords: Magnetic interaction, Magnetorheological suspensions, Magnetoactive polymers, Dipole models

1. Introduction

Magnetorheological (MR) or soft magnetic elastomer (SME) is a polymer matrix filled with microparticles of a ferromagnet or ferrite. Mechanical properties of such composites change considerably in response to applied magnetic fields, and this is the main cause of practical interest to those systems. Under an external field, the magnetostatic forces between the filler particles emerge which strive to re-arrange the inner structure of the composite. This, in turn, changes the macroscopic rheological properties of SMEs: the storage modulus, the intrinsic friction coefficient, etc. Due to that, the problem of interparticle magnetic forces is an essential issue of fundamental and applied magnetomechanics of SMEs.

Conventional SMEs are filled with micron-size magnetic dispersions. A typical case is carbonyl iron with 1–10 μm grains, see [1-4]. This is a magnetically soft material with the initial susceptibility $\chi_0 \sim 10^3 - 10^5$ emu, whose magnetization saturates under a field of few kOe [5]. Therefore, a reference iron microparticle does not have any spontaneous magnetic moment. In a weak field it acquires magnetic moment μ growing linearly with the field, while in a strong field μ tends to a constant value, i.e., saturates.

To describe the particle interaction in the presence of a static field \mathbf{H}_0 most often point dipole models are used. This kind of approximation implies that the interparticle distances by far exceed the reference particle size, so that the magnetic field and magnetization inside each particle might be treated as uniform. If one adopts for the ferromagnet a linear isotropic magnetization law, $\mathbf{M} = \chi_0 \mathbf{H}$, then the magnetic moment of a particle of

volume V may be written as $\mu = \int \mathbf{M} dV = \mathbf{M}V = \chi_0 \mathbf{H}V$.

For an isolated spherical particle, the strength of internal field is determined solely by the strength of the applied one, as $\mathbf{H} = \mathbf{H}_0 - (4\pi/3)\mathbf{M} = \mathbf{H}_0 - (4\pi/3)\chi_0 \mathbf{H}$, and for the particle magnetic moment one has

$$\mu = \frac{\chi_0}{1 + \frac{4\pi}{3}\chi_0} \mathbf{H}_0 V. \quad (1)$$

A magnetized dipolar particle is a source of its own field, which is defined by well-known expression [6]:

$$\mathbf{H}_d = -\frac{\mu}{r^3} + 3\frac{(\mu \cdot \mathbf{r})\mathbf{r}}{r^5}, \quad (2)$$

where r is the length of radius-vector \mathbf{r} of an arbitrary point in the surrounding space.

Consider two dipolar particles subjected to an external field. The energy of this pair consists of two terms: the energy of interaction with the applied field (the doubled Zeeman energy of an isolated particle) and the interaction energy. The latter has the form [6]:

$$U_{12} = \frac{\mu_1 \cdot \mu_2}{l^3} - 3\frac{(\mu_1 \cdot \mathbf{l})(\mu_2 \cdot \mathbf{l})}{l^5}, \quad (3)$$

where \mathbf{l} is the center-to-center vector connecting particles 1 and 2. Using definition $\mathbf{f} = -\nabla U$, from Eq. (3) one gets a formula for the interparticle force:

$$\mathbf{f} = -\frac{\partial U}{\partial \mathbf{l}} = -\frac{3(\boldsymbol{\mu}_1 \cdot \boldsymbol{\mu}_2)\mathbf{l}}{l^5} - \frac{3(\boldsymbol{\mu}_1 \cdot \mathbf{l})\boldsymbol{\mu}_2}{l^5} - \frac{3(\boldsymbol{\mu}_2 \cdot \mathbf{l})\boldsymbol{\mu}_1}{l^5} + \frac{15(\boldsymbol{\mu}_1 \cdot \mathbf{l})(\boldsymbol{\mu}_2 \cdot \mathbf{l})\mathbf{l}}{l^7}, \quad (4)$$

which is convenient to present as a sum of two components as

$$\mathbf{f} = \mathbf{f}_n + \mathbf{f}_\tau, \quad \mathbf{f}_n = -\frac{\mathbf{l}}{l^2} \left(\mathbf{l} \cdot \frac{\partial U}{\partial \mathbf{l}} \right), \quad \mathbf{f}_\tau = \frac{1}{l^2} \left(\mathbf{l} \times \left(\mathbf{l} \times \frac{\partial U}{\partial \mathbf{l}} \right) \right). \quad (5)$$

Thus one sees that the particle attraction / repulsion is determined by the central force \mathbf{f}_n directed along vector \mathbf{l} , while \mathbf{f}_τ characterizes the force couple tending to align the interparticle vector \mathbf{l} with the applied field.

The basic convenience and advantage of the dipole models is that they ensure pair-wise interaction. In this case, calculation of energy for a multiparticle system reduces to summation over all the possible pairs. Right because of that, the dipolar approach became and still remains the main investigation “tool” in the theory of electro- and magnetorheological suspensions and in the theory of magnetic elastomers as well. In the present paper, taking a pair of particles as a simplest representative element of an MR system, we compare the existing variants of dipolar models with each other and with the exact numerical solutions. For the case of iron-based SMEs, a new model is proposed, which is capable to determine the effect of the ferromagnet saturation on the interparticle forces.

2. Linear interacting dipoles (LID model)

The general criterion of the point-dipole model applicability is $l \gg a$, where a is the particle radius. This means that the particles are so remote that the difference in interaction between their closest and farthest elements is negligible. Therefore, with respect to magnetic interactions, a particle of finite size, even if its internal magnetization distribution is non-uniform, is characterized by means of a single vector, the magnetic dipole moment $\boldsymbol{\mu}$. The magnetic field induced by a dipole is rendered by Eq. (2). This field diminishes with the distance by power law, i.e., is long-ranged. Due to that, the force experienced by a given particle is determined by the joint dipole field \mathbf{H}_{loc} , which is induced at the point of particle location by all the other members of the assembly. For a magnetizable (polarizable) particle the value of its own magnetic moment $\boldsymbol{\mu}$ is a function of the combined field $\mathbf{H}_{ext} = \mathbf{H}_0 + \mathbf{H}_{loc}$.

Adding to the above-stated assumptions a hypothesis that the particle substance magnetizes according to the linear law $\mathbf{M} = \chi_0 \mathbf{H}$, one arrives at the *linear interacting dipoles* (LID) model [7,8]. Evidently, the particles considered in the framework of LID model are virtually

(super)paramagnetic, for ferromagnet particles this model might be valid only in a weak field limit.

Let us apply the LID model to a simplest representing element of a MR composite: a set of two spherical particles of the same radius a . Since the particles are identical in their magnetic properties, they as well possess coinciding magnetic moments $\boldsymbol{\mu}_1 = \boldsymbol{\mu}_2 = \boldsymbol{\mu}$ and, thus, induce equal dipolar fields $\mathbf{H}_{loc1} = \mathbf{H}_{loc2} = \mathbf{H}_d$.

The point-dipole approximation is equivalent to the assumption that the particle magnetization is uniform, so that $\boldsymbol{\mu} = \mathbf{M}V$. In the problem under study, each particle is subjected to the external field $\mathbf{H}_{ext} = \mathbf{H}_0 + \mathbf{H}_d$, which induces the internal field

$$\mathbf{H} = \mathbf{H}_{ext} - (4\pi/3)\mathbf{M} = \mathbf{H}_0 + \mathbf{H}_d - (4\pi/3)\mathbf{M}. \quad (6)$$

Substituting here \mathbf{H}_d from (2), one arrives at the set of equations in the form

$$A_{ik} \mathbf{H}_k = \mathbf{H}_{0i}, \quad A_{ik} = \left[1 + \frac{\chi_0 V}{l^3} + \frac{4\pi\chi_0}{3} \right] \delta_{ik} - 3\chi_0 V \frac{l_i l_k}{l^5}, \quad (7)$$

where δ_{ik} is unit tensor.

Solution of Eqs. (7) yields the internal field strength \mathbf{H} according to the LID model. Using it, one is able to, first, find the magnetic moments of the particles and, then, to evaluate their dipole interaction energy:

$$U_{12} = -\boldsymbol{\mu} \cdot \mathbf{H}_0 = -\chi_0 V \mathbf{H} \cdot \mathbf{H}_0. \quad (8)$$

To calculate the interparticle force from Eq. (8), we use Eq. (7) that ties up the strengths of external and internal fields. The result takes the form

$$(\mathbf{f})_i = -\left(\frac{\partial U}{\partial l_i} \right) = -\left(\frac{\partial}{\partial l_i} (\boldsymbol{\mu} \cdot \mathbf{H}_0) \right)_i = -\chi_0 V \frac{\partial}{\partial l_i} (H_k H_{0k}) = -\chi_0 V \left(H_k \frac{\partial A_{kl}}{\partial l_i} H_l \right). \quad (9)$$

As seen, differentiation of energy with respect to vector \mathbf{l} reduces to taking a derivative of tensor A_{ik} in (7). Carrying out these simple calculations and returning to the notation $\boldsymbol{\mu} = \chi_0 V \mathbf{H}$, one arrives at expression

$$\mathbf{f} = -\frac{3}{l^5} \left[\mu^2 - \frac{5}{l^2} (\boldsymbol{\mu} \cdot \mathbf{l})^2 \right] \mathbf{l} - \frac{6}{l^5} (\boldsymbol{\mu} \cdot \mathbf{l}) \boldsymbol{\mu}, \quad (10)$$

which coincides with that obtained by differentiating the energy of a pair of dipoles with permanent magnetic moments (4). Thus, we have proven that the expression for the pair interparticle force preserves its form independently of whether the particle magnetic moments are spontaneous (permanent) or field induced. Right this

assumption was used by the authors of Refs. [7,8] when constructing their LID models.

Following Eq. (5), we split the force (10) in two components

$$\begin{aligned} f_n &= \frac{3\mu^2 l}{l^5} - \frac{9(\mu \cdot l)^2 l}{l^7}, \\ f_\tau &= -\frac{6(\mu \cdot l)^2 l}{l^7} + \frac{6(\mu \cdot l)\mu}{l^5}, \end{aligned} \quad (11)$$

and compare the predictions on those functions given by a simple LD model (dipoles do not affect each other), the LID model and the exact solution, which fully takes into account mutual polarization of the particles [9]. In Fig. 1, this comparison is done for the reference iron particles with $\chi_0 = 10^3$ emu. Fig. 1a shows the central force f_n for the head-to-tail pattern, i.e., zero angle γ between vectors \mathbf{l} and \mathbf{H}_0 ; Fig. 1b presents the angle dependence of the tangential force f_τ .

As seen, the more the particles approach one another (Fig. 1a) or the more the angle γ tends to 45° (Fig. 1b) the greater the LD and LID models deviate from the exact solution. However, the LID model works a bit better. This is proven by Fig. 2, where the relative errors evaluated against the exact solution are given. Fig. 2 also establishes that the deviations of the dipole models from the exact solution are the smaller the lower is the particle magnetic susceptibility. The parameters at panes b) and c) of Fig. 2 refer to two real systems. Pane b) characterizes the

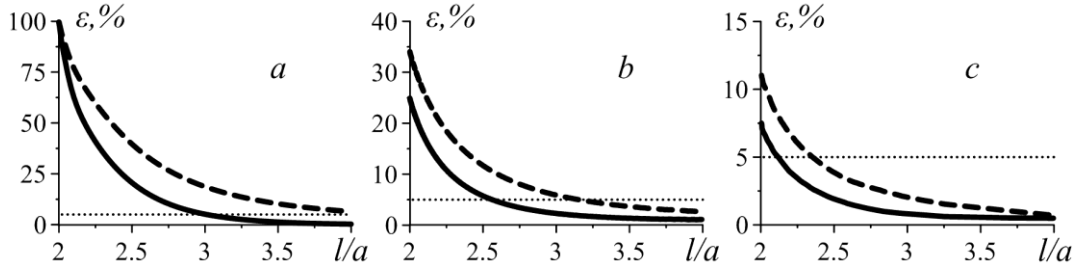


Fig. 2. Central force f_n evaluation errors with the LD (dashes) and LID (solid line) models in the $\gamma = 0$ configuration; the magnetic susceptibility $\chi_0 = 10^3$ (a); 0.08 (b); 0.02 emu (c).

3. Nonlinear interacting dipoles (NID model)

As mentioned, in ferromagnets the magnetization law resembles the linear one only in weak-to-moderate fields. With the increase of the field strength (for iron, up to few kOe), the particle magnetization increase, first, slows down and then stops: the particle enters the magnetization saturation regime. To describe such a behavior, one has to introduce a field-dependent magnetic susceptibility: $\mathbf{M} = \chi(\mathbf{H})\mathbf{H}$. Since typical MR composites are filled with iron, we take the nonlinear magnetization law in the Frölich-Kennelly (FK) form [5,11,12], presenting it in nondimensional units as

Dynabead microspheres with susceptibility $\chi_0 = 0.08$ emu as reported in Ref. [8]; pane c) describes the superparamagnetic microspheres with susceptibility $\chi_0 = 0.02$ emu studied in Ref. [10]. Obviously, for the objects with low magnetic susceptibility even simple models might apply fairly well.

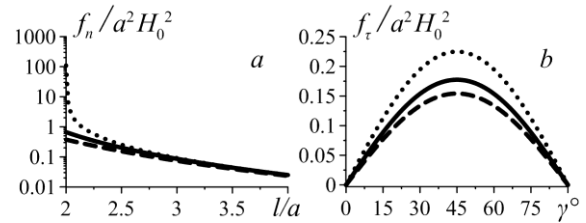


Fig. 1. Interparticle forces from the LD model (dashes), LID model (solid lines) and from the exact solution (points); pane (a): the central force f_n at $\gamma = 0$; pane (b): the angle dependence of the tangential force f_τ ; the interparticle distance is $l = 2.1a$, the magnetic susceptibility is $\chi_0 = 10^3$ emu.

Note also that in the paramagnetic approximation (constant χ_0) all the forces grow quadratically with the field strength ($f \propto H_0^2$). Because of that, under appropriate scaling, like that used at the ordinate axes in Fig. 1, the obtained dependences are universal.

$$\mathbf{m} = \frac{\chi_0 \mathbf{h}}{\chi_0 \mathbf{h} + 1}, \quad \mathbf{h} = \frac{\mathbf{H}}{M_s}, \quad \mathbf{m} = \frac{\mathbf{M}}{M_s}; \quad (12)$$

As seen, the FK ferromagnet has the initial susceptibility χ_0 , while under strong field its magnetization tends to M_s (saturation).

For dilute MR systems ($l \ll a$), the interaction of nonlinearly magnetizable particles might be described neglecting their reciprocal polarization. The only difference from the linear case is that the internal field is now found from equation

$$\mathbf{h} = \mathbf{h}_0 - \frac{4\pi}{3} \frac{\chi_0 \mathbf{h}}{\chi_0 h + 1}. \quad (13)$$

As the mutual influence of the particles is considered as insignificant, the directions of vectors \mathbf{h} and \mathbf{h}_0 coincide, Eq. (13) becomes quadratic with respect to h . It has two solutions, one of which is unphysical. Discarding it, one gets the field strength inside the particle in the form

$$h = \frac{\sqrt{36\chi_0 h_0 + (4\pi\chi_0 - 3\chi_0 h_0 + 3)^2}}{6\chi_0} - \frac{(4\pi\chi_0 - 3\chi_0 h_0 + 3)}{6\chi_0}. \quad (14)$$

The magnetization curve $m(h_0)$ of an isolated particle obtained from Eqs. (12) and (14) is shown in Fig. 3; for $\chi_0 = 10^3$. As seen, in this case the magnetization crossover (transition from quasi-linear regime to saturation) takes place in a narrow interval around $h_0 = 4\pi/3$. In a pair of particles, the same behavior should be inherent to the energy and to the interparticle force.

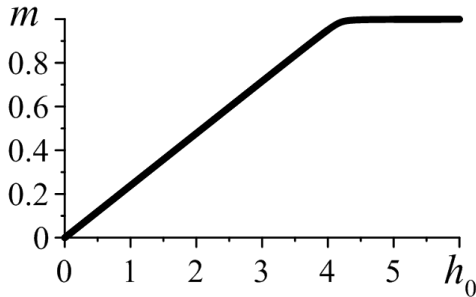


Fig. 3. Magnetization of an isolated particle with initial susceptibility $\chi_0 = 10^3$ as a function of the external field strength.

To evaluate the energy of a pair of magnetizable particles we use the general formula [6]:

$$\tilde{U} = \frac{U}{M_s^2} = -V \left[\mathbf{m} \cdot (\mathbf{h} - \mathbf{h}_0) - 2 \int_0^h \mathbf{m} \cdot d\mathbf{h} \right]. \quad (15)$$

Substituting there the internal field from Eq. (14) and then subtracting the doubled energy of an isolated particle, one gets the proper interaction energy of the dipolar pair. Differentiation of this energy according to Eq. (5) yields the interaction forces \mathbf{f}_n and \mathbf{f}_τ , which—as it is easy to show—coincide with the force components (4), i.e., with the result of direct differentiation of the dipolar energy.

Formulas (12)-(14) define the simplest model describing pair interaction of nonlinearly magnetizable dipolar particles. We term it ND-model, and it in a natural way extends the above-introduced LD-model. Carrying on

the analogy, we construct the *nonlinear interacting dipoles* (NID model). The field strength inside each of the particles is determined similarly to the linear case (6) with the only difference that $\chi(h)$ is now field-dependent. With allowance for saturation, the set (7) becomes nonlinear but does not change its general form:

$$\begin{aligned} A_{ik} h_k &= h_{0k}, \\ A_{ik} &= \left[1 + \frac{\chi(h)V}{l^3} + \frac{4\pi\chi(h)}{3} \right] \delta_{ik} - 3\chi(h)V \frac{l_i l_k}{l^5}. \end{aligned} \quad (16)$$

Taking function $\chi(h)$ from the FK law (13), the set (16) is easily solvable numerically. To evaluate the interparticle forces, one may—following the standard procedure—substitute the found field strength \mathbf{h} in the energy (15) and then take the derivative with respect to \mathbf{l} . However, much easier is to immediately use formula (4) for the interaction force.

Fig. 4 presents the dependence of the attraction/repulsion forces on the external field for four orientations of the pair: $\gamma = 0, 45^\circ, 60^\circ, 90^\circ$. The curves are obtained with the aid of the models of interacting linear and nonlinear dipoles (LID and NID) and the non-interacting nonlinear dipoles model (ND); here, as in above, the value $\chi_0 = 10^3$ is used.

As seen, in the ND model the saturation regime indeed occurs in the vicinity of $h_0 = 4\pi/3$. In the NID model, the situation is different. In the head-to-tail pattern, the field induced by the adjacent particle enhances the field inside the given one, while in the side-by-side orientation the effect of reciprocal magnetization is negative. Due to that, the particle pair aligned with the field ($\mathbf{l} \parallel \mathbf{h}_0$) saturates easier than that in the perpendicular configuration ($\mathbf{l} \perp \mathbf{h}_0$), cf. Figs. 4a and 4d. For the cases of pairs in tilted orientations (Figs. 4b and 4c), the central force attains maximum at the saturation point and decreases afterwards.

The force maxima in Fig. 4 are inherent only to the particles, whose magnetization saturates and, hence, could be understood only in the framework of the NID model. Let us clarify the origin of this effect. Note that the particle internal field \mathbf{h} is proportional to the vector sum of the external field \mathbf{h}_0 and the field \mathbf{h}_d induced by the adjacent dipole, see Eq. (6). In the linear and quasi-linear regimes of magnetization, the particle magnetic moment (and, thus, its contribution to \mathbf{h}_d and to the magnetization of the neighbor particle) grows mostly in magnitude keeping the direction virtually constant. Hereupon, the attraction force goes up with the field, see Figs. 4b and 4c. In the saturation regime, the particle magnetic moments become constant in length and are able only to rotate. This means that in the sum (6), which determines orientation of vector

μ , the second and third terms virtually stop to change in absolute values. Meanwhile, the external field keeps growing. As a result, the internal field vector \mathbf{h} and, consequently, the particle magnetic moment align more and more with the external field, i.e., the angle θ between μ and \mathbf{h}_0 diminishes. The corresponding function $\theta(h_0)$ is shown in Fig. 5. It also displays crossover behavior: the angle θ remains virtually constant until the field attains a certain value but afterwards asymptotically goes down to zero.

The plots of Fig. 4 correspond to the center-to-center distance $l = 2.1a$. At this value of the gap, the linearly magnetizable particles attract each other in the angle interval $0 \leq \gamma < 75^\circ$ [9]. If the saturation regime is on, and the magnetic moments are independent of the applied field, then the particle interaction might be described with the model of permanent dipoles [13]. For those, the orientation angle interval of attraction is independent of l and ranges $0 < \gamma < 54.7^\circ$, i.e., is substantially narrower than that for magnetizable particles. This fact explains, why for the pair with $\gamma = 45^\circ$ the interaction in strong fields remains attractive (Fig. 4b), while for the pair with $\gamma = 60^\circ$ the field growth turns the interaction into repulsion (Fig. 4c).

Let us compare the dependence of force f_n on the interparticle distance as predicted by different models. In Fig. 6 this is done for configuration $\gamma = 0^\circ$. In undersaturating fields (Fig. 6a) the results of LID and NID models (dotted and solid lines) are very close. In the intermediate field range (Fig. 6b) the dependence yielded by the NID model (solid line) is fairly well approximated by the ND model (dashes), in high fields these models virtually coincide (Fig. 6c).

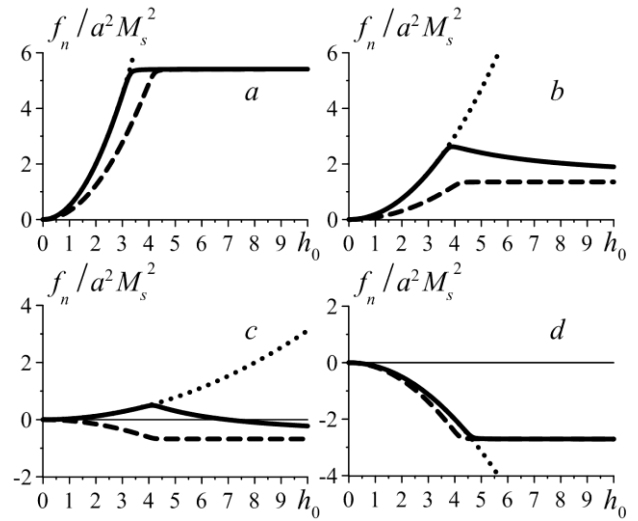


Fig. 4. Central force for $l = 2.1a$ under variation of the pair orientation: $\gamma = 0^\circ$ (a), 45° (b), 60° (c), 90° (d); the model results are: ND (dashes), LID (points), NID (solid line).

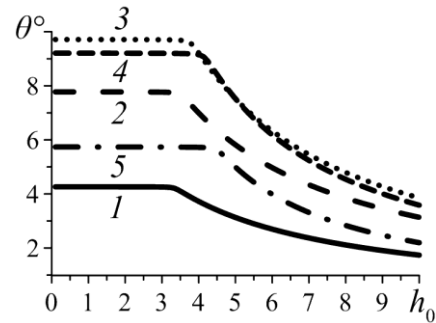


Fig. 5. The angle θ between the external field \mathbf{h}_0 and magnetic moment μ for $l = 2.1a$ as a function of h_0 for the pair orientations: $\gamma = 15^\circ$ (1), 30° (2), 45° (3), 60° (4) and 75° (5).

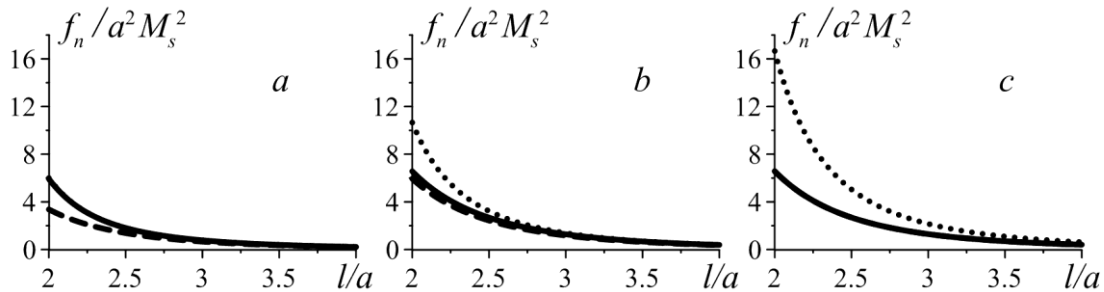


Fig. 6. Central force f_n for $\gamma = 0$ as a function of the interparticle distance according to the LID model (dots), ND model (dashes), and NID model (solid line) under the fields $h_0 = 3$ (a), 4 (b), 5 (c).

4. Interparticle forces with allowance for magnetization saturation

As known, a pair of dipole particles subjected to a uniform external field experiences mutual attraction in the head-to-tail pattern and repulsion in the side-by-side geometry. For the case of permanent point dipoles, the central force f_n inverses its sign (attraction to repulsion) when the angle γ exceeds 54.7° and this boundary value does not depend neither on the interparticle distance nor on the applied field strength. In the case of magnetizable particle such dependences readily emerge.

In Fig. 7a a pair of particles is schematically presented, the origin of the coordinate framework is set at the center of particle 1. Under close contact distance ($l = 2a$), the center of particle 2 is positioned on the arc plotted by thick dashes. The examples of other isolines $l = \text{const}$ are drawn by dashed arcs. The neutral curves in Fig. 7a, which go approximately radially, are the loci of

the points where $f_n = 0$ as given by the NID model. The region above a neutral curve corresponds to particle attraction, the area below it—to their repulsion. The straight line that goes under the angle $\gamma_0 \approx 55^\circ$ to the vertical axis, shows the neutral line for permanent point dipoles.

The neutral lines for the LID model are not shown but they, as expected, closely follow those of the NID model in the field-range below saturation ($h_0 < 4\pi/3$). In this field range the shift of the neutral curve and the width of the angle interval of attraction are maximal. For example, at $h_0 = 4$ and upon the particle contact, the angle interval of attraction is $0 \leq \gamma \leq 64.6^\circ$. The width of this interval as a function of external field is shown in Fig. 7b for the interparticle distances l corresponding to the radii of the arcs in Fig. 7a. For linearly magnetizable particles in contact, the exact solution predicts the widest interval: $0 \leq \gamma \leq 84^\circ$ [9].

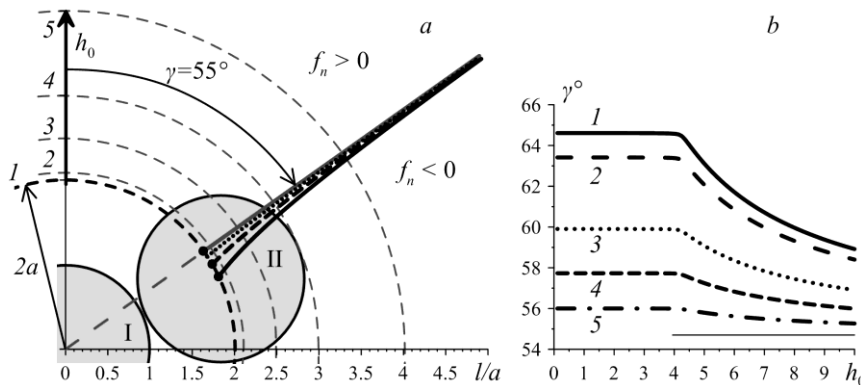


Fig. 7. The results of the NID model: a) the approximately radial lines at the schematic view of the pair are neutral curves ($f_n = 0$) for $h_0 = 4$ (solid line), 8 (dashes), 20 (points); b) the width of the attraction angle interval as a function of the applied field strength for center-to-center distances $l = 2a$ (1), $2.1a$ (2), $2.5a$ (3), $3a$ (4), $4a$ (5).

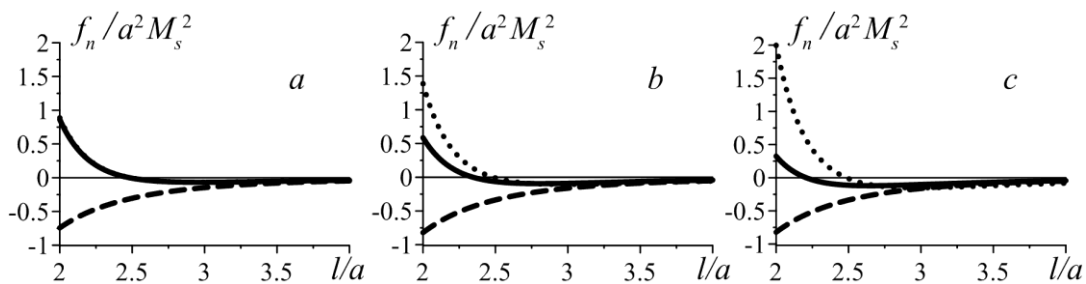


Fig. 8. Central force f_n as a function of the center-to-center distance at $\gamma = 60^\circ$ in the field $h_0 = 4$ (a), 5 (b), 6 (c); LID model (points), ND model (dashes), NID model (solid line).

In Fig. 8 the dependence of f_n on the center-to-center distance is presented for $\gamma = 60^\circ$ and for several values of the external field. All the curves rendered by the ND model are located beneath the abscissa axis that implies mutual repulsion of the particles. The forces predicted by the LID model change sign at a fixed interparticle distance whatever the applied field. Below transition to saturation ($h_0 = 4$),

the force predicted by the NID and LID models coincide. However, with the field growth, the differences between LID and NID enhance, and this deviation is accompanied by reduction of the interparticle distance at which the force inversion takes place.

The effect of magnetic saturation on the tangential interparticle force is somewhat unexpected. Saturation

turns out to be a factor that breaks the angle symmetry of function $f_\tau(\gamma)$. We remind that for permanent dipoles as well as in LD, LID and ND models, the dependence of the pair energy on the angle γ comes out exactly as $\cos^2 \gamma$ [14-17]. Thus, for the tangential force in either model one has $f_\tau \propto \sin 2\gamma$. The particles whose magnetization saturates, lack such universality. The NID model enables one to reveal this effect and to estimate its magnitude, see Figs. 9 and 10. As follows from them, the maximum of f_τ shifts to greater angles the stronger the higher the field h_0 and the shorter is the distance between the dipoles.

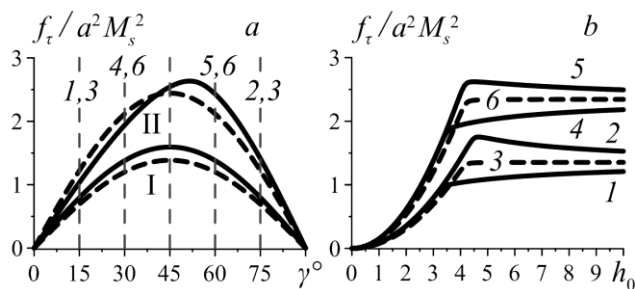


Fig. 9. Tangential force f_τ for $l = 2.1a$: a) as a function of angle in the field $h_0 = 3$ (I) and 4 (II); ND model (dashes), NID model (solid lines); b) as a function of external field, dashes show the results of the ND model for $\gamma = 15^\circ$ and 75° (3), $\gamma = 30^\circ$ and 60° (6); solid lines correspond to the NID model for $\gamma = 15^\circ$ (1) and 75° (2), 30° (4) and 60° (5).

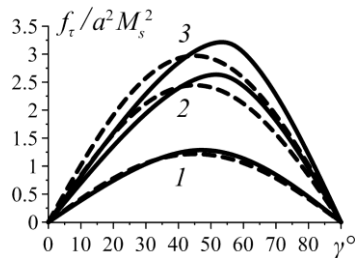


Fig. 10. Angle dependence of f_τ at $h_0 = 4$ for the center-to-center distances $l = 2.5a$ (1), $2.1a$ (2), $2a$ (3); the ND model (dashes), the NID model (solid lines).

As follows from Fig. 9a, the ND model in the under-saturation fields renders equal values of f_τ for the particle pairs with the orientation angles equally remote from $\gamma = 45^\circ$; for example, $\gamma = 30^\circ$ and 60° . However, due to the anisotropy of magnetic interactions, the dipoles in the first configuration saturate at lower field than those in the second one. As shown in Fig. 9b, the particle interaction in a pair with $\gamma < 45^\circ$ keeps growing (solid curves 1 and 4) and approaches the limiting value (established by the ND model) from beneath. In the configurations where $\gamma > 45^\circ$ this force, on attaining maximum, goes down and tends to the same limit from above (solid curves 2 and 5).

5. Discussion and conclusions

The results of comparing various models employed for describing magnetic interaction between ferromagnet microparticles are described.

Magnetic saturation is an effect that takes control over the mechanical characteristics of MR composites in the moderate-to-strong field range. It is an issue of high interest in the corresponding science and technology. This problem had been to some extent addressed with regard to MR suspensions, where iron microparticles readily crowd together when a field is imposed. In MR polymers the situation is different since the particles sit in an elastic environment that prevents their massive crowding. So, for magnetized MR polymers more typical is formation of groups of just few particles, the case, about which quite a little is known both in theory and experiment.

In the present work, we take as a representing element of a MR elastomer a set of two identical spherical particles. To account for the fact that typically the MR systems are filled with microdisperse iron, the magnetic constitutive equation for the particle substance is taken in the FK form.

Even a two-particle problem with allowance for magnetic saturation becomes nonlinear and could be solved in full only numerically requiring big spends of computer resources. However, as our analysis shows, the true numerical solution is really necessary only under sufficiently strong fields. In the field range below the saturation region the solution with admissible accuracy (less than 5%) might be obtained assuming that the particles magnetize linearly, and the latter problem has analytical solutions [14-17]. Another occasion, where a simple solution is acceptable is the case of sufficiently dilute dispersion. Here, depending on the values of interparticle distance l and the applied field strength h_0 , one may use one of the dipolar models.

The diagram indicating the ranges where a specific model suffices to characterize the particle pair that occupies head-to-tail configuration, i.e., has $\gamma = 0$, is presented in Fig. 11. This map is plotted as a result of comparison of approximate and numerical data. The parameter plane $(h_0, l/a)$ is divided in six regions, and in four of them (regions 3-6) one of the above-discussed dipole models suffices to evaluate the interparticle forces with accuracy better than 5%.

Regions 1 and 2 in Fig. 11 do not admit any dipolar approximation. In region 1 the particles neighbor each other so closely that the internal field strength in each of them is around the saturation level, i.e., the function $m(h)$ is highly nonlinear. Due to that, the result could be obtained only by numerical solution of a nonlinear magnetostatic problem. In region 2, although the internal field is below saturation, the closeness of the particles entails the necessity to take into account not only the dipole but the higher multipole contributions to the interaction as well. This is done by summing up [9] the multipole series derived analytically, see [15].

The NID model proposed in this paper, “takes care” of an important region on the diagram of Fig. 11, viz. the particles in nearly tight contact ($l/a \approx 2$) in the field interval $3.5 < h_0 < 4.5$, where the magnetization saturation occurs in full. Without this new model, all this area would have been accessible only with the aid of numeric solution. Usefulness and predictive ability of the NID model is demonstrated by discovering (i) the non-monotonic dependence of the central force on the applied field and (ii) the angle symmetry breakdown of the tangential force f_τ . It is worth noting that in the past in the course of numerical work we have encountered certain manifestations of those peculiarities. However, at that time we did not have explanations for them. The NID model, having simplified substantially the analysis of interparticle magnetic forces, provided clear proofs that the above-mentioned nonlinear effects originate from the particle magnetic saturation.

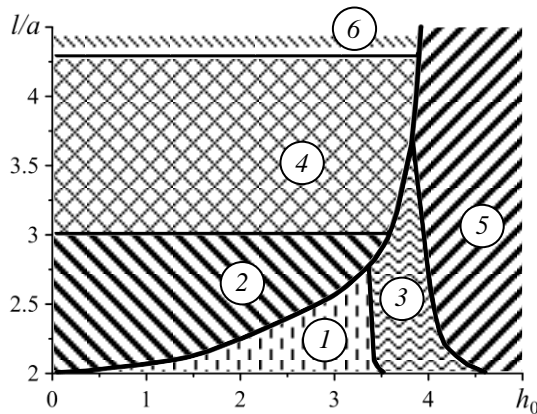


Fig. 11. Model applicability diagram (accuracy better than 5%) for the dipole models in the case $\gamma = 0$: nonlinear numerical solution is required (1), linear multipole solution is required (2), NID applies (3), LID applies (4), ND applies (5), LD applies (6).

The diagram of Fig. 11 describes the situation only for $\gamma = 0$. Evidently, when the angle γ changes, the boundaries would deform. Not presenting here the plots for non-zero γ , we remark in this connection that since in the side-by-side pattern ($\gamma = 90^\circ$) the fields of neighboring particles weaken each other, then the regions of validity of the models should extend in comparison with the configuration $\gamma = 0$. This would diminish the area of region 1, thus enhancing the range of applicability of the dipole models.

It is worthwhile to remark that although the FK model is a well-known and trusted approximation for iron, it is by no means a unique one. We employ it here for two main reasons. First, it is very simply parametrized and, thus, convenient for calculations. Second, it possesses the essential feature of any magnetically soft ferromagnet: the anhysteretic nonlinear magnetization curve. Evidently, other models of saturating magnetization could be used with their own $M(H)$ curves inherent to the particle material. Such a replacement would with necessity shift

quantitatively the force and energy dependences against those presented here. However, all the qualitative features of the field-induced behavior revealed with the aid of the FK model, would remain the same. In other words, the NID model provides a kind of “framework” that would readily work with any nonlinear magnetization law ascribed to the material in question.

Acknowledgements

The work was done under auspices of RFBR grants 13-01-96056 and 14-02-96003 and of project S26/617 supported by Ministry for Education and Science of Perm Region.

References

- [1] M. R. Jolly, J. D. Carlson, B. D. Muñoz, T. A. Bullions, *J. Intelligent Materials, Systems and Structures* **7**, 613 (1996).
- [2] L. V. Nikitin, L. S. Mironova, G. V. Stepanov, and A. N. Samus, *Polymer Science, Ser. A* **43**, 443 (2001).
- [3] J. M. Ginder, S. M. Clark, W. F. Schlotter, M. E. Nichols, *Int. J. Modern Physics B* **16**, 2412 (2002).
- [4] M. Lokander and B. Stenberg, *Polymer Testing* **22**, 245 (2003).
- [5] R. M. Bozorth, *Ferromagnetism*, Wiley-IEEE Press, (1993).
- [6] L. D. Landau, E. M. Lifshitz, and L. P. Pitaevskii, *Electrodynamics of Continuous Media*. 2nd ed. Press, New York (1984).
- [7] E. E. Keaveny and M. R. Maxey, *J. Computational Physics* **227**, 9554 (2008).
- [8] D. Du, F. Toffoletto, and S. L. Biswal, *Physical Review E* **89**, Art. no. 043306 (2014).
- [9] A. M. Biller, O. V. Stolbov, and Yu. L. Raikher, *J. Applied Physics* **116**, Art. no. 114904 (2014).
- [10] M. N. Romodina, M. D. Khokhlova, E. V. Lyubin, and A. A. Fedyanin, *Scientific Reports* **5**, Art. no. 10491 (2015).
- [11] C. H. Lee, F. Reitich, M. R. Jolly, T. Banks, and K. Ito, *IEEE Transactions on Magnetics* **37**, 558 (2001).
- [12] G. Bossis, P. Khuzir, S. Laci, and O. Volkova, *J. Magnetism and Magnetic Materials* **258-259**, 456 (2003).
- [13] V. N. Bagaev, Yu. A. Buyevich, and V. V. Tetyukhin, *Magnetohydrodynamic* **22**, 146 (1986).
- [14] D. K. Ross, *Australian J. Physics* **21**, 817 (1968).
- [15] D. J. Jeffrey, *Proc. Roy. Soc. (London) Ser. A* **335**, 355 (1973).
- [16] D. J. Klingenberg, C. F. Zukoski, *Langmuir* **6**, 15 (1990).
- [17] H. J. H. Clercx, G. Bossis, *Physical Review E* **48**, 27121 (1993).

*Corresponding author: kam@icmm.ru